High frequency dielectric properties of $A_5B_4O_{15}$ microwave ceramics

S. Kamba,[a] J. Petzelt, E. Buixaderas, D. Haubrich, and P. Vaněk
Institute of Physics, Academy of Sciences of the Czech Republic, Na Slovance 2, 182 21 Prague, Czech Republic

P. Kužel
Institute of Physics, Academy of Sciences of the Czech Republic, and Center for Complex Molecular Systems and Biomolecules, Na Slovance 2, 182 21 Prague, Czech Republic

I. N. Jawahar and M. T. Sebastian
Regional Research Laboratory, Trivandrum 695 019, India

P. Mohanan
Department of Electronics, CUSAT, Cochin 682 022, India

(Received 29 September 2000; accepted for publication 4 January 2001)

High-frequency dielectric properties of $A_5B_4O_{15}$ (A=Ba, Sr, Mg, Zn, Ca; B=Nb, Ta) dielectric ceramics are studied by means of the microwave cavity technique, a combination of far-infrared reflection and transmission spectroscopy and time-resolved terahertz transmission spectroscopy. Microwave permittivity ϵ' and $Q\times f$ factor vary, depending on the chemical composition, between 11 and 51, and 2.4 and 88 THz, respectively. The temperature coefficient τ_f varies between -73 and 232 ppm/°C, and in two samples $|\tau_f|$ is less than 15 ppm/°C. It is shown that the microwave permittivity ϵ' of the ceramics studied is determined by the polar phonon contributions and that linear extrapolation of the submillimeter dielectric loss ϵ'' down to the microwave region is in agreement with the microwave data of single phase samples. The relationship among phonon spectra, the crystal structure, and the unit cell volume is discussed. © *2001 American Institute of Physics.* [DOI: 10.1063/1.1351873]

I. INTRODUCTION

Recent progress in microwave (MW) telecommunications has demanded the need for good quality ceramic dielectric resonators. The important characteristics required for dielectric resonators are high permittivity ϵ' (the size of resonators is proportional to $1/\sqrt{\epsilon'}$), a high quality factor $Q=\epsilon'/\epsilon''$, and a low temperature coefficient of resonant frequency τ_f. Unfortunately, these requirements cannot be fulfilled simultaneously. High ϵ' materials generally have higher dielectric loss ϵ'' (lower Q) and frequently also high τ_f.[1] The method of sample preparation has a pronounced influence on the value of ϵ'' in the MW region, while ϵ' is almost insensitive to it. MW losses can vary by several orders of magnitude between samples of the same chemical composition but with different amounts of defects.[2] Usually, technologists try to reduce ϵ'' empirically. Then, it is not clear whether extrinsic losses are completely eliminated and the intrinsic value of ϵ'' is achieved. In this case spectroscopic methods, which directly access the far infrared (FIR) and submillimeter (SMM) spectral regions, i.e., classical FIR spectroscopy and time-domain terahertz transmission spectroscopy (TDTTS),[3] appear to be powerful methods for direct estimation of the intrinsic losses not only in FIR but also in the MW region, because the intrinsic ϵ'' is simply proportional to the frequency well below the phonon frequencies ($f\leqslant 10^{12}$ Hz).[4] As early as 1962, Ruprecht and Bell[5] experimentally confirmed that the relation $\epsilon''(\omega)\propto\omega$ is fulfilled in $SrTiO_3$. The same frequency dependence can be theoretically obtained from the formula,[6]

$$\epsilon^*(\omega)=\epsilon'(\omega)-i\epsilon''(\omega)=\sum_{j=1}^{n}\frac{\Delta\epsilon_j\omega_{\mathrm{TO}j}^2}{\omega_{\mathrm{TO}j}^2-\omega^2+i\omega\gamma_{\mathrm{TO}j}}+\epsilon_\infty, \tag{1}$$

in the limit $\omega\ll\omega_{\mathrm{TO}j}$. Equation (1) describes the complex dielectric function $\epsilon^*(\omega)$ as a sum of classical harmonic oscillators with eigenfrequencies $\omega_{\mathrm{TO}j}$, dampings $\gamma_{\mathrm{TO}j}$, and oscillator strengths $\Delta\epsilon_j\omega_{\mathrm{TO}j}^2$. ϵ_∞ denotes high-frequency permittivity originating from electron transitions. Each oscillator describes an optical polar phonon mode contributed by $\Delta\epsilon_j$ to the static dielectric permittivity. The limit $\omega\ll\omega_{\mathrm{TO}j}$ also yields frequency independent permittivity $\epsilon'=\Sigma\Delta\epsilon_j+\epsilon_\infty$ in the MW and SMM regions.

Wakino *et al.* used the above method for the determination of $\epsilon''(\omega)$ in the MW region from infrared reflectivity spectra of $Ba(Zr,Zn,Ta)O_3$ ceramics.[4] The complex dielectric response can be obtained from reflectivity using the Kramers–Kronig relations or by fitting the reflectivity to Eq. (1) and[7]

$$R(\omega)\equiv\left|\frac{\sqrt{\epsilon^*(\omega)}-1}{\sqrt{\epsilon^*(\omega)}+1}\right|^2. \tag{2}$$

However, FIR reflectivity spectra have limited sensitivity to the weak modes in the SMM region (10–100 cm^{-1}), and, therefore, we have extended this method and used a combi-

[a]Electronic mail: kamba@fzu.cz

nation of FIR reflection and a more sensitive FIR transmission spectroscopy in the SMM region for the determination of MW losses in many materials.[1,2,8] An accurate determination of $\epsilon^*(\omega)$ in the SMM region is very important for its extrapolation down to the MW region. The above mentioned techniques give $\epsilon^*(\omega)$ only from the model fit of the spectra, hence it is very useful to combine the FIR spectroscopy with TDTTS which can typically access the range of 3–80 cm^{-1}, and is phase sensitive. This can provide, independently, both real and imaginary parts of the permittivity without any fitting models.[9]

Many defects such as porosity, grain boundaries, microcracks, etc. can reduce the proportionality range between ϵ'' and the frequency.[2] The presence of a second phase may cause even additional peaks in ϵ'' in the SMM region.[2] On the other hand, theory[10] shows that not only intrinsic losses due to multiphonon absorption, but also extrinsic losses by charged-defect induced one-phonon absorption of acoustic branches, yield $\epsilon''(\omega) \propto \omega$. Nevertheless, extrinsic losses can be well distinguished from intrinsic ones from the temperature dependences. The latter should decrease upon cooling and disappear at low temperatures near liquid He temperature.[1,10]

In this article we focus on investigation of a material family $A_5B_4O_{15}$ (A=Ba, Sr, Mg, Zn, Ca; B=Nb, Ta) with ϵ' up to 51. Until now only $Ba_5Nb_4O_{15}$ and $(Ba_{5-x}Sr_x)Nb_4O_{15}$ ceramics were investigated from the point of view of MW properties.[11–14] It was shown that the pure compounds for $x=0$ and 5 have permittivity values of 38 and 40, respectively, while solid solutions have enhanced permittivity up to 51 with high $Q \times f$ up to 24 THz. These promising properties stimulated us to investigate $A_5B_4O_{15}$ ceramics with different chemical compositions (A=Ba, Sr, Mg, Zn, Ca; B=Nb, Ta).

The crystal structure is known for six studied compounds only: $Ba_5Ta_4O_{15}$, $Sr_5Ta_4O_{15}$, and $Ba_5Nb_4O_{15}$ crystallize in trigonal space group D_{3d}^3-P3m1 $(Z=1)$.[15–18] Monoclinic symmetry C_{2h}^1-P2/m with $Z=2$ (Ref. 19) was reported for $Sr_5Nb_4O_{15}$, but a very recent paper[20] also confirmed trigonal symmetry D_{3d}^4-P3c1 with $Z=2$. The c parameter is doubled due to antitilting of TiO_6 octahedra ($\sim 15°$) around the c axis.[20] The structure of all four of the above mentioned compounds consists of five AO_3 close-packed layers with B ions located in corner-sharing octahedral holes between the layers. No B atom lies between the third and the fourth layers.[15,17,19] The crystal structure of $Mg_5Nb_4O_{15}$ and $Mg_5Ta_4O_{15}$ is completely different and is isostructural with pseudobrookite Fe_2TiO_5.[21] The space group is orthorhombic $D_{2h}^{17}-Cmcm$ with $Z=4$. The structure consists of double chains of $(Mg,B)O_6$ units, sharing edges of the bc plane, interconnected through common oxygen along the a axis to give a three-dimensional array.[21]

IR reflectivity and Raman-scattering spectra of $Ba_5Nb_4O_{15}$ were published in 1996 by Massa *et al.*[22] According to these authors the spectra indicate that the lattice of this compound is close to collapse into a lower symmetry structure. MW properties, x-ray diffraction, Raman scattering, and FIR transmission spectra of $Ba_{5-x}Sr_xNb_4O_{15}$ were published by Ratheesh *et al.*[14] Their data did not support the monoclinic symmetry of $Sr_5Nb_4O_{15}$ suggested by Weiden *et al.*[19] According the authors' knowledge, the remaining three materials ($5ZnO-2Nb_2O_5$, $5CaO-2Nb_2O_5$, and $5CaO-2Ta_2O_5$), which are studied in this article, have not been characterized by means of any physical method.

II. EXPERIMENT

All the $A_5B_4O_{15}$ ceramics were prepared by the conventional solid-state ceramic route. The respective high purity carbonates or oxides were used as the starting materials. The $Mg_5Nb_4O_{15}$ and $Mg_5Ta_5O_{15}$ were prepared using as-received MgO and also using MgO heated at 1000 °C for 3 h. Raw MgO powder is hydrated and carbonated from the air, i.e., it contains magnesium carbonate and/or hydroxide.[23] The starting carbonate/oxide powders were stoichiometrically weighed to get a gross amount of about 20 g, mixed thoroughly in an agate mortar using distilled water or acetone as the wetting medium for 1 h, dried and again mixed for 1 h. The reaction mixtures for the niobates were calcined at 1050–1275 °C whereas those for tantalates were calcined at 1200–1400 °C for 4–10 h depending on the materials. The calcined powders were ground well for 1 h, mixed with 5 wt % PVA solution, which acts as a suitable binder, dried, and again ground for 1 h. The fine powders were uniaxially pressed into green pellets of 5–6 or 9–10 mm in length, with diameters of 11 mm, under a pressure of 150 MPa. Stearic acid (2 wt %) dissolved in isopropyl alcohol was used as a lubricant within the die. The green pellets were sintered by placing them on a platinum plate at optimum temperatures between 1220 and 1610 °C for 4 h. The optimum sintering temperature is taken as the temperature at which the density is found to be a maximum. The densities of the sintered pellets were measured using the Archimedes method. The pellets were well polished to remove any irregularities on the flat surfaces of the pellets before performing the MW measurements.

An HP 8510C network analyser and an HP 8514 reflection-transmission test unit interfaced with a computer were used for the MW characterization. The cylindrical dielectric resonators were positioned and shorted between two brass plates and the TE_{011} mode was identified. ϵ' was determined from the frequency of the TE_{011} mode and the dimensions of the samples using the Hakki–Coleman method.[24] τ_f was obtained by heating the sample in a temperature range of 25–75 °C and noting the temperature variation of the resonant frequency of the TE_{011} mode. The Q factor of the sample at the $TE_{01\delta}$ mode was measured by the Khanna–Garault stripline method.[25] The structure and homogeneity of the samples were studied using a Philips PW 1710 x-ray diffractometer.

IR reflectivity and transmission spectra were obtained at room temperature using a Fourier transform spectrometer (Bruker IFS 113 v) in the frequency ranges of 30–2000 and 15–100 cm^{-1} (0.45–3 THz), respectively. The resolution of the reflectivity spectra was 2 cm^{-1}, although accurate determination of the interferences in the transmission spectra required a resolution of 0.5 cm^{-1}. Room temperature deuterated triglicin sulfate (DTGS) detectors were used for the reflectivity measurements, while a highly sensitive, helium

TABLE I. Sintering temperature, density, permittivity ϵ', quality factor Q multiplied by resonance frequency f, and temperature coefficient τ_f of resonance frequency of the ceramics investigated.

Material	Sintering temperature (°C)	Density	Density (%)	ϵ'	$Q\times f$ (GHz)	τ_f (ppm/°C)
$Mg_5Ta_4O_{15}$	1550	6.47	...[b]	17	2000×7.19	−15
$Mg_5Ta_4O_{15}$[a]	1560	5.56	91	11	2000×9.06	−54
$Sr_5Ta_4O_{15}$	1610	7.00	96	41	400×5.99	...[c]
$Ba_5Ta_4O_{15}$	1550	7.63	95	28	5700×5.55	12
$Mg_5Nb_4O_{15}$	1475	4.20	...[b]	14	2000×7.28	−58
$Mg_5Nb_4O_{15}$[a]	1450	3.90	94	11	4500×8.30	−54
$Ba_5Nb_4O_{15}$	1380	6.07	96	39	5000×4.73	78
$Ba_4SrNb_4O_{15}$	1400	5.64	92	48	3100×4.70	140
$Ba_3Sr_2Nb_4O_{15}$	1400	5.44	93	50	3500×4.71	232
$Ba_2Sr_3Nb_4O_{15}$	1400	5.41	95	51	4600×4.61	117
$BaSr_4Nb_4O_{15}$	1400	5.46	95	45	5100×4.57	82
$Sr_5Nb_4O_{15}$	1400	5.20	93	40	4000×4.84	55
$5ZnO-2Nb_2O_5$	1220	5.61	...[b]	21	12 600×6.98	−73
$5CaO-2Ta_2O_5$	1550	6.25	...[b]	41	1000×5.90	140
$5CaO-2Nb_2O_5$	1500	4.20	...[b]	32	1000×6.48	−37

[a]Prepared from MgO powder heat treated at 1000 °C for 3 h.
[b]Density could not be evaluated due to the multiphase nature of the sample.
[c]τ_f could not be measured due to poor resonance.

cooled (1.5 K) Si bolometer was used for the transmission measurements.

The experimental setup of TDTTS uses a biased large-aperture antenna (low-temperature grown GaAs) as a terahertz emitter and an electro-optic sampling detection technique. It is described in detail elsewhere.[9]

Disk-shaped samples, with diameters of 9 mm and thicknesses of 1–2 mm, were used for the reflectivity measurements. Plane parallel (about 200 ± 1 μm) thin plates were prepared for transmission measurements.

III. RESULTS AND DISCUSSION

A. XRD analysis and MW dielectric properties

A list of all materials studied together with their MW parameters is shown in Table I. The recorded x-ray diffraction (XRD) data of $Ba_5Ta_4O_{15}$, $Ba_5Nb_4O_{15}$, and $Sr_5Ta_4O_{15}$ ceramics agree well with earlier reports[15] that give information about single phase compositions. The $Mg_5Nb_4O_{15}$ and $Mg_5Ta_4O_{15}$ ceramics prepared using as-received MgO powder show good sinterability and density, but XRD revealed the presence of additional secondary phases of $MgTa_2O_6$ and $MgNb_2O_6$, respectively. The samples prepared using the heat-treated MgO show single phase $Mg_5Nb_4O_{15}$ and $Mg_5Ta_4O_{15}$ with lower ϵ' (=11) and the same $\tau_f(=-54\,\text{ppm/°C})$. Lee *et al.*[26] have reported that $MgTa_2O_6$ has a high Q factor ($Q\times f=59\,600$ GHz) and high ϵ' (30.3) and positive $\tau_f(+30\,\text{ppm/°C})$. The presence of $MgTa_2O_6$ as a secondary phase in $Mg_5Ta_4O_{15}$ caused an increase in ϵ' and the positive τ_f of $MgTa_2O_6$ favorably shifts the τ_f of the nonhomogeneous $Mg_5Ta_4O_{15}$ to −17 ppm/°C according to the mixing rule.[27] $MgNb_2O_6$ has $\epsilon'=21.4$, $Q\times f=93\,800$ GHz, and $\tau_f=-70$ ppm/°C.[26] Again, the presence of $MgNb_2O_6$ as the secondary phase in $Mg_5Nb_4O_{15}$ is the reason for the increased ϵ', $Q\times f$, and τ_f of the $Mg_5Nb_4O_{15}$ prepared using the raw MgO. The lack of magnesium in the unheated MgO favors the growth of $MgNb_2O_6$ and $MgTa_2O_6$ secondary phases. Hence heating of MgO is a critical requirement for obtaining single phase ceramics of the above mentioned compounds. Only multiphase samples of $Mg_5Nb_4O_{15}$ and $Mg_5Ta_4O_{15}$ were investigated by means of FIR and TDTTS techniques.

Due to the absence of any data on $5ZnO-2Nb_2O_5$, $5CaO-2Nb_2O_5$, and $5CaO-2Ta_2O_5$ systems, the XRD analysis became difficult. The diffractograms obtained were compared with those phases that are expected to occur in the system. We found that the expected compounds did not form under the present preparation conditions. $5ZnO-2Nb_2O_5$ ceramics contain $ZnNb_2O_6$ and $Zn_3Nb_2O_8$ as the major phases. The columbite phase $ZnNb_2O_6$ is reported to have high $\epsilon'=25$, τ_f of −56 ppm/°C and $Q\times f$ of 83 700 GHz.[26] The diffraction peaks of $5CaO-2Nb_2O_5$ ceramics can be indexed by assuming $Ca_2Nb_2O_7$ and $Ca_3Nb_2O_8$ are the phases formed. $CaTa_2O_6$ and $Ca_2Ta_2O_7$ are found to be possible phases in $5CaO-2Ta_2O_5$ ceramic as revealed by XRD. The $CaTa_2O_6$ has an eschynite cubic structure and $\epsilon'=21.2$, $\tau_f=1$ ppm/°C, and $Q\times f=11\,600$ GHz.[26] Details of the structural and microstructural characterization of all samples obtained by XRD and scanning electron microscopy will be published elsewhere.

B. Infrared and submillimeter spectra

IR reflectivity spectra of all the investigated ceramics together with the fits are shown in Fig. 1. Many samples show broad reflection bands, i.e., they exhibit large splitting of longitudinal optic (LO) ω_{LOj} and transverse optic (TO) ω_{TOj} phonon frequencies. In this case their corresponding dampings γ_{LOj} and γ_{TOj} could substantially differ. Therefore, instead of Eq. (1) we have used the generalized factorized four-parameter oscillator model of the complex permittivity,[7]

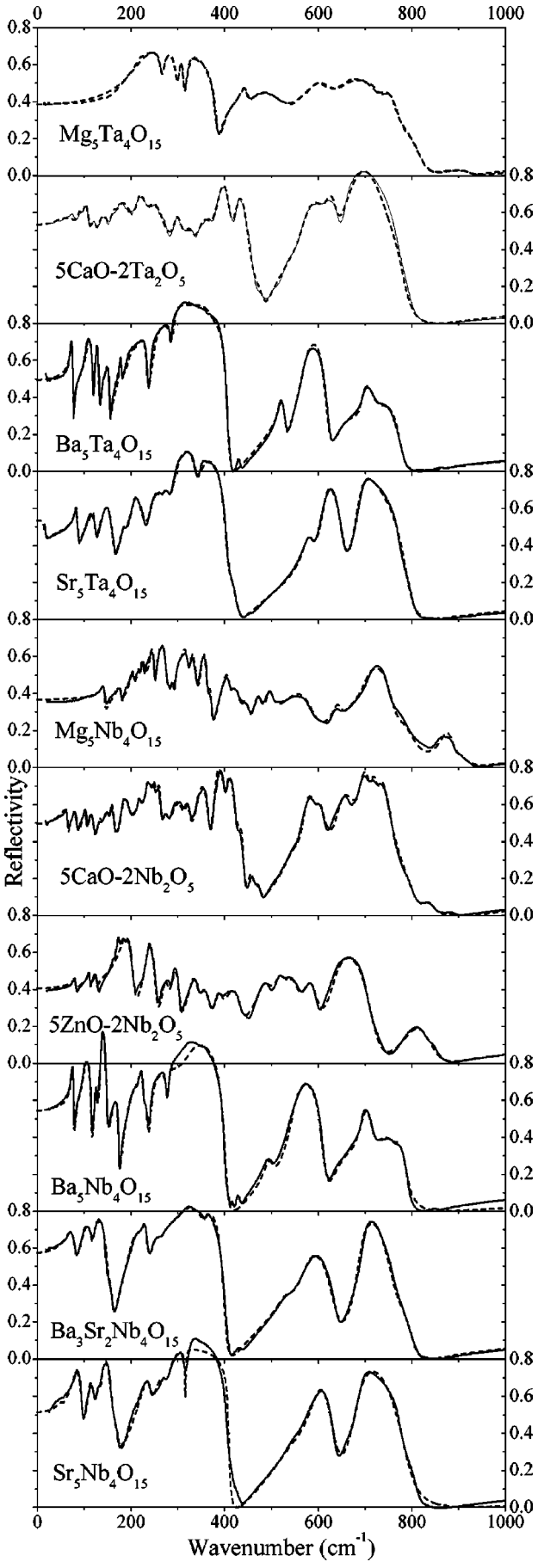

FIG. 1. IR reflectivity spectra of the ceramics investigated. Solid and dashed curves are experimental and fitted curves, respectively.

$$\epsilon^*(\omega)=\epsilon_\infty\prod_j\frac{\omega_{\mathrm{LO}j}^2-\omega^2+i\omega\gamma_{\mathrm{LO}j}}{\omega_{\mathrm{TO}j}^2-\omega^2+i\omega\gamma_{\mathrm{TO}j}}. \tag{3}$$

All the reflectivity spectra were fitted together with the transmission spectra. The reason for the simultaneous fitting was that in many cases the parameters of a good reflectivity fit did not fit the transmission spectra satisfactorily. Hence, in these cases we have added to the fit a weak and highly damped oscillator roughly describing the multiphonon absorption below the phonon frequencies. These weak additional features have no influence on reflectivity fits (reflectivity is not sensitive to weak absorption processes), but they markedly improved the transmission fit. The method of calculation of $\epsilon^*(\omega)$ from the transmission spectra is described elsewhere.[28]

$\epsilon'(\omega)$ and $\epsilon''(\omega)$ obtained from the above fits were compared with the time-resolved THz spectra and the MW data; see Figs. 2 and 3. One can see that the experimental $\epsilon'(\omega)$ points agree very well with the calculated curves (obtained from reflectivity and transmission fits). No dispersion of $\epsilon'(\omega)$ is seen below the phonon frequencies; very good agreement of SMM ϵ' with the values in the MW region is observed. The accuracy of $\epsilon'(\omega)$ obtained through TDTTS is very high and depends practically only on the precision of the sample thickness determination. Experimental SMM values of $\epsilon''(\omega)$ are noisier than permittivity $\epsilon'(\omega)$ because of lower sensitivity of the method in the case of low dielectric loss at low frequencies. The error bars are shown at the high and low frequency parts of the spectra if they exceed the size of the points. Most of the experimental $\epsilon''(\omega)$ values correspond to the calculated curves within experimental error. Some deviation is seen, but mostly in cases of multiphase samples. The linear extrapolation of SMM dielectric losses agrees rather well with the experimental MW data. Nevertheless, without cooling the samples we cannot say which kind of losses (extrinsic or intrinsic) predominate. Phonon spectra can also help us to distinguish which sample is single phase and which is not.

C. Phonon spectra and crystal structure

There is a close relationship between the features in IR reflectivity spectra and the crystal structure of the ceramics investigated. The number of atoms(s) in the primitive unit cell determines the number of different phonon modes N ($N=3s$) in the Brillouin zone (BZ) center (Γ point of the BZ). Not all optical phonons are infrared active, but the crystal structure determines the symmetry of vibrations and their activities in IR and Raman spectra.

$Ba_5Ta_4O_{15}$, $Sr_5Ta_4O_{15}$, and $Ba_5Nb_4O_{15}$ crystallize in the trigonal space group D_{3d}^3 with one formula unit ($Z=1$) per unit cell.[15–18] In this case 72 Γ-point modes are expected. Factor group analysis yields $A_{2u}+E_u$ acoustic modes (E_u is doubly degenerate) and $8A_{1g}(x^2+y^2,z^2)+2A_{2g}+10E_g(x^2-y^2,xy,xz,yz)+3A_{1u}+10A_{2u}(z)+13E_u(x,y)$ optical modes in the Γ point of the BZ.[22] The letters in parentheses give the mode activities in the spectra: x^2, xy, xz, etc. represent Raman activity in corresponding symmetry spectra; x,y,z indicate infrared activity of the modes in $E\|x$, $E\|y$,

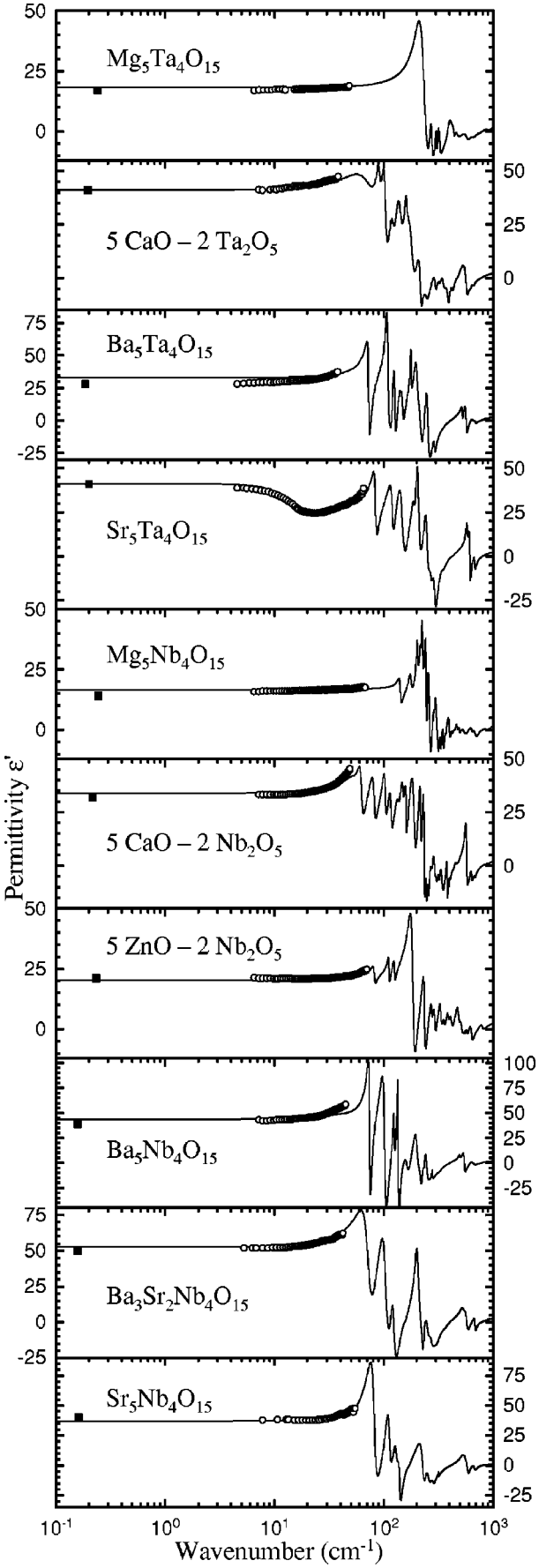

FIG. 2. Permittivity ϵ' obtained from the fit of FIR transmission and reflectivity spectra (solid lines) compared with experimental values from the MW resonant cavity method (closed squares) and TDTTS measurements (open circles).

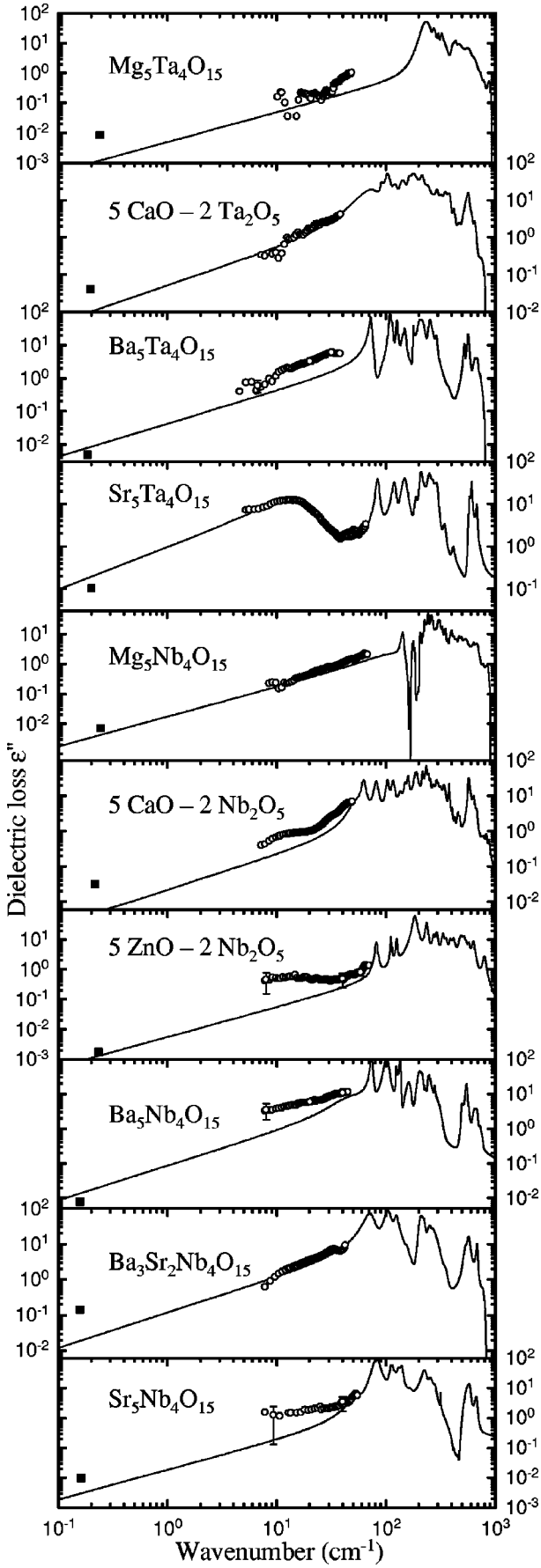

FIG. 3. Dielectric loss ϵ'' obtained from the MW resonant cavity method (closed squares) and TDTTS measurements (open circles) compared with the result of the fit of FIR transmission and reflectivity spectra (solid lines). Note the log–log scale.

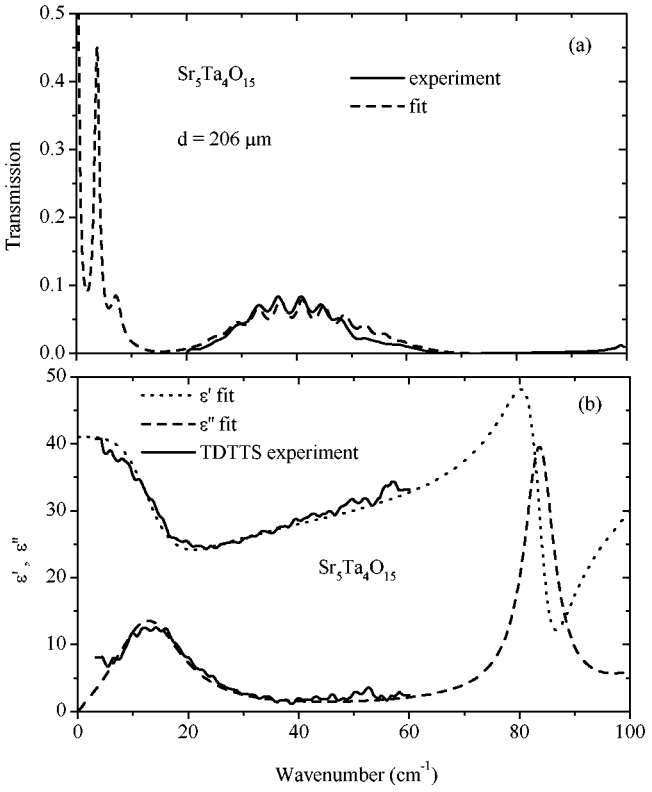

FIG. 4. (a) Experimental and fitted FIR transmission spectra of $Sr_5Ta_4O_{15}$. (b) Complex dielectric spectra obtained from the TDTTS measurement compared with the result of FIR transmission and reflectivity fits.

and $E\|z$ polarized spectra, respectively. In the ceramics, the symmetry of the $13E_u$ and $10A_{2u}$ modes cannot be distinguished in the IR spectra because of averaging over all grain orientations. Therefore all 23 modes may be expected in the IR spectra. Our fits of $Ba_5Ta_4O_{15}$ and $Ba_5Nb_4O_{15}$ ceramics spectra yield 17 and 18 phonon modes, respectively. It is a rather common case that not all predicted modes are seen in the spectra; the phonons can be weak or heavily damped in room temperature (RT) spectra and reflection bands can be overlapped. The spectra of $Ba_5Nb_4O_{15}$ agree very well with the spectra published by Massa *et al.*[22]

$Sr_5Ta_4O_{15}$ exhibits unusual low frequency heavily damped excitation at 15 cm^{-1}. This mode is partially seen in the reflectivity and is very well evident in both THz and FIR transmission spectra (see Fig. 4). The excellent agreement of the TDTTS experiment with the result of FIR transmission and reflectivity spectra fits is noticeable and illustrates the accuracy of our measurements. If the $Sr_5Ta_4O_{15}$ sample contains traces of a second phase with a complicated structure (more formula units per unit cell), the folded acoustic phonons could become IR active at such a low frequency. However, our XRD measurement confirmed only a single phase composition. So the absorption peak at 15 cm^{-1} is probably due to a phonon and its frequency is so low that it could be a soft optical mode. This could indicate lattice instability and the possibility of a ferroelectric phase transition. However, our differential scanning calorimetry (DSC) (Perkin-Elmer DSC 7) did not reveal any phase transition in the range of 95–920 K. Low temperature dielectric measurement below 95 K is needed for the detection of a possible ferroelectric phase transition.

Two structures were reported for $Sr_5Nb_4O_{15}$, monoclinic and trigonal. If the sample would crystallize in the monoclinic space group C_{2h}^1 with $Z=2$,[19] the factor group analysis yields A_u and $2B_u$ acoustic modes and $39A_g(x^2,y^2,z^2,xy) + 30A_u(z) + 27B_g(xz,yz) + 46B_u(x,y)$ optical modes. It means that totally 76 phonon modes could be expected in IR spectra. If the sample crystallizes in the recently reported D_{3d}^4 space group with $Z=2$,[20] the group analysis yields $A_{2u}+E_u$ acoustic modes and $11A_{1g}(x^2+y^2,z^2)+13A_{2g} + 24E_g(x^2-y^2,xy,xz,yz) + 11A_{1u} + 12A_{2u}(z)+23E_u(x,y)$ optical modes in the Γ point of the BZ. So, overall 35 optical modes can be expected in the IR spectra. In our case, only 13 modes were sufficient for the reflectivity spectra fitting, so the trigonal structure of the sample is more probable. Again, not all symmetry allowed modes are seen in the spectra due to their overlapping and high damping. Our result is consistent with the conclusion of Ratheesh *et al.*,[14] who also failed to confirm the monoclinic structure of $Sr_5Nb_4O_{15}$ with $Z=2$. One can see that the spectra of $Ba_{5-x}Sr_xNb_4O_{15}$ are very similar to those of pure compounds with $x=0$ and 5, so the structure of $Sr_5Nb_4O_{15}$ seems to be similar to $Ba_5Nb_4O_{15}$ with $Z=1$. Phonon dispersion branches of optical phonons probably have only small dispersion in the BZ. The newly activated modes in the folded BZ have similar frequencies as the already active modes, hence they are not resolved in reflectivity spectra and only effectively higher damping of most of the modes is observed.

The reflectivity spectra of $Mg_5Ta_4O_{15}$ and $Mg_5Nb_4O_{15}$ are completely different from previously discussed spectra, giving evidence about the different crystal structure. Both materials crystallize in the orthorhombic D_{2h}^{17} space group with $Z=4$ in the centered unit cell.[21] Their chemical formula can be rewritten as $Mg_{5/3}B_{4/3}O_5$ (B=Nb or Ta) in order to be compared with the stoichiometry of the pseudobrookite Fe_2TiO_5. Necessarily, there must be a mixed occupancy of both metal positions, so the most general formula is $(Mg_{1-m}B)_{4c}(Mg_{2/3+m}B_{4/3-m})_{8f}O_5$ in which both $4c$ and $8f$ positions are occupied by both cations Mg(II) and Nb(V) or Ta(V), randomly distributed.[21] The group analysis yields $B_{1u}+B_{2u}+B_{3u}$ acoustic modes and $8A_g(x^2,y^2,z^2)+3A_u + 5B_{1g}(xy) + 7B_{1u}(z) + 3B_{2g}(xz) + 7B_{2u}(y) + 8B_{3g}(yz) + 4B_{3u}(x)$ optical modes. It means that only 18 IR active modes are expected in the spectra of orthorhombic ceramics with pseudobrookite structure. Fourteen modes were observed in the reflectivity spectrum of $Mg_5Ta_4O_{15}$, however, 28 modes are distinguished in the $Mg_5Nb_4O_{15}$ spectrum, giving evidence about the traces of a second phases in the sample.

The IR reflectivity spectrum of $5ZnO-2Nb_2O_5$ ($Zn_5Nb_4O_{15}$) with 18 modes is very similar to the $Mg_5Nb_4O_{15}$ spectrum, and manifests the multiphase composition of the ceramics. XRD measurement revealed that the ceramics contain $ZnNb_2O_6$ and $Zn_2Nb_3O_8$ as the major phases. The $5CaO-2Nb_2O_5$ ($Ca_5Nb_4O_{15}$) and $5CaO-2Ta_2O_5$ ($Ca_5Ta_4O_{15}$) also display completely different reflectivity spectra compared with other samples, supporting the results of XRD measurements that the ceramics do not

form single phases but consist also of phases like CaB_2O_6, $Ca_2B_2O_7$, etc. (B=Nb, Ta). The multiphase composition of the ceramics is probably also responsible for their rather low Q.

IV. CONCLUSIONS

New MW dielectrics with a general chemical formula $A_5B_4O_{15}$ (A=Ba, Sr, Mg, Zn, Ca; B=Nb, Ta) were studied by means of the MW resonant cavity technique, FIR reflection, transmission, and TDTTS. The last technique allowed us to determine directly ϵ' and ϵ'' in the range of 5–60 cm^{-1}(0.15–1.8 THz). The experimental THz data correspond very well to the results of the fits of FIR transmission and reflection spectra. Some exceptions are seen only in multiphase samples. It is shown that the MW ϵ' of our ceramic samples is determined by the polar phonon contributions and therefore ϵ' is dispersionless below the phonon frequencies. In single phase samples, dielectric loss ϵ'' extrapolated from the SMM down to the MW regions according to the simple proportionality $\epsilon''(\omega) \propto \omega$ corresponds satisfactorily to the MW data. The number of phonon modes observed in IR reflectivity spectra reveals information about the symmetry of the crystal structure of the ceramics investigated, particularly about the number of formula units in the primitive unit cell. The spectra of $Ba_5Nb_4O_{15}$, $Ba_5Ta_4O_{15}$, and $Sr_5Ta_4O_{15}$ support the same trigonal symmetry with $Z=1$. The low frequency excitation at 15 cm^{-1} in $Sr_5Ta_4O_{15}$ suggests a ferroelectric soft mode; however, low temperature measurements are needed. The IR spectrum of $Sr_5Nb_4O_{15}$ does not support the previously published report of monoclinic symmetry with $Z=2$. The spectrum is similar to that for the three related samples with trigonal symmetry and $Z=1$. Spectra of $Mg_5Nb_4O_{15}$ and $Mg_5Ta_4O_{15}$ confirm the known pseudobrookite structure; however, the higher number of modes in $Mg_5Nb_4O_{15}$ indicate some traces of a second phase in the sample. The spectra of $5ZnO-2Nb_2O_5$. $5CaO-2Nb_2O_5$, and $5CaO-2Ta_2O_5$ differ from the spectra of all the above investigated samples because of their multiphase compositions.

ACKNOWLEDGMENTS

This work was supported by the Grant Agency of the Czech Republic (Project Nos. 202/98/1282 and 202/98/P022) and the Grant Agency of the Academy of Sciences of the Czech Republic (Project No. A1010828) and by the Defence Research and Developement Organisation (DRDO), New Delhi. One of the authors (I.N.J.) is grateful to the Council of Scientific and Industrial Research (CSIR), New Delhi, for the award of a research fellowship.

[1] J. Petzelt, S. Kamba, G. V. Kozlov, and A. A. Volkov, Ferroelectrics **176**, 145 (1996).
[2] S. Kamba, J. Petzelt, R. Freer, V. M. Ferreira, R. Zurmühlen, and V. Koukal, *Proceedings of the International Conference on Electronic Ceramics and Applications*, edited by J. L. Babtista, J. A. Labrincha, and P. M. Vilarinho (University of Aveiro Press, Aveiro, 1996), Vol. 2, p. 63.
[3] D. 3, S. Keiding, M. van Exter, and Ch. Fattinger, J. Opt. Soc. Am. B **7**, 2006 (1990).
[4] K. Wakino, D. A. Sagala, and H. Tamura, Jpn. J. Appl. Phys., Part 1 **24**, 1042 (1985); K. Wakino, M. Murata, and H. Tamura, J. Am. Ceram. Soc. **69**, 34 (1986).
[5] G. Ruprecht and R. O. Bell, Phys. Rev. **125**, 1915 (1962).
[6] J. Petzelt and N. Setter, Ferroelectrics **150**, 89 (1993).
[7] F. Gervais, in *Infrared and Millimetre Waves*, edited by K. J. Button (Academic, New York, 1983), Vol. 8, Chap. 7, p. 279.
[8] J. Petzelt *et al.*, Ferroelectrics **93**, 77 (1989).
[9] P. Kužel and J. Petzelt, Ferroelectrics **239**, 79 (2000).
[10] V. L. Gurevich and A. K. Tagantsev, Adv. Phys. **40**, 719 (1991).
[11] H. Sreemoolanadhan, J. Isaac, S. Solomon, M. T Sebastian, K. A. Jose, and P. Mohanan, Phys. Status Solidi A **143**, K45 (1994).
[12] C. Vineis, P. K. Davies, T. Negas, and S. Bell, MRS Bull. **31**, 431 (1996).
[13] H. Sreemoolanadhan, M. T Sebastian, and P. Mohanan, MRS Bull. **30**, 653 (1995).
[14] R. Ratheesh, H. Sreemoolanadhan, and M. T. Sebastian, J. Solid State Chem. **131**, 2 (1997).
[15] F. Galasso and L. Katz, Acta Crystallogr. **14**, 647 (1961).
[16] J. Shannon and L. Katz, Acta Crystallogr., Sect. B: Struct. Crystallogr. Cryst. Chem. **26**, 102 (1970).
[17] J. L. Hutchison, Chem. Scr. **14**, 181 (1978–79).
[18] S. Pagola, G. Polla, G. Leyva, M. T. Casais, J. A. Alonso, I. Rasines, and R. E. Carbonio, Mater. Sci. Forum **228**, 819 (1996).
[19] M. Weiden, A. Grauel, J. Norwig, S. Horn, and F. Steglich, J. Alloys Compd. **218**, 13 (1995).
[20] N. Teneze, D. Mercurio, G. Trolliard, and J. C. Champarnaud-Mesjard, Z. Kristallogr. **215**, 11 (2000).
[21] S. Pagola, R. E. Carbonio, M. T. Fernandez-Diaz, and J. A. Alonso, J. Solid State Chem. **137**, 359 (1998).
[22] N. E. Massa, S. Pagola, and R. Carbonio, Phys. Rev. B **53**, 8148 (1996).
[23] S.-H. Ra and P. P. Phule, J. Mater. Res. **14**, 4259 (1999).
[24] B. W. Hakki and P. D. Coleman, IRE Trans. Microwave Theory Tech. **8**, 402 (1970).
[25] A. P. S. Khanna and Y. Garault, IEEE Trans. Microwave Theory Tech. **31**, 261 (1983).
[26] H. J. Lee, I.-T. Kim, and K. S. Hong, Jpn. J. Appl. Phys., Part 2 **36**, L1318 (1997).
[27] A. J. Moulson and J. M. Herbert, *Electroceramics* (Chapman and Hall, London, 1990), p. 79.
[28] A. A. Volkov, Yu. G. Goncharov, G. V. Kozlov, S. P. Lebedev, and A. M. Prokhorov, Infrared Phys. **25**, 369 (1985).